AGU PUBLICATIONS

Geophysical Research Letters

RESEARCH LETTER
10.1002/2016GL067738

Key Points:
- Spatial-temporal patterns of hydrological droughts derived from limited data in the Amazon basin
- Droughts in northern and southern subbasins differ in trends and association to climatic indices
- Trend toward more intense droughts in southern subbasins is linked to Atlantic Ocean anomalies

Supporting Information:
- Supporting Information S1
- Data Set S1
- Data Set S2
- Data Set S3
- Data Set S4

Correspondence to:
A. V. Lopes,
alanvazlopes@berkeley.edu

Citation:
Lopes, A. V., J. C. H. Chiang, S. A. Thompson, and J. A. Dracup (2016), Trend and uncertainty in spatial-temporal patterns of hydrological droughts in the Amazon basin, *Geophys. Res. Lett.*, *43*, 3307–3316, doi:10.1002/2016GL067738.

Received 20 JAN 2016
Accepted 16 MAR 2016
Accepted article online 21 MAR 2016
Published online 6 APR 2016

Trend and uncertainty in spatial-temporal patterns of hydrological droughts in the Amazon basin

A. V. Lopes[1], J. C. H. Chiang[2], S. A. Thompson[3], and J. A. Dracup[3]

[1]National Water Agency, Brasilia, Brazil, [2]Department of Geography, University of California, Berkeley, California, USA, [3]Department of Civil and Environmental Engineering, University of California, Berkeley, California, USA

Abstract Spatial-temporal patterns of hydrological droughts in the Amazon basin are derived from drought indices computed from existing streamflow data. Principal component analysis and Monte Carlo simulations are employed to account for the uncertainty and overcome the limitations of missing data in streamflow records. Results show that northern and southern subbasins differ in drought trends and in patterns of correlation between drought indices and climate anomalies originating from the Pacific (El Niño–Southern Oscillation) and Atlantic (differences in sea surface temperature across the equator) Oceans. A significant trend toward more intense droughts is found in the southern subbasins, which is highly correlated to tropical Atlantic Ocean sea surface temperature anomalies. That drying trend might have distinct causes in each subbasin and can lead to potential intensification of regional impacts.

1. Introduction

Streamflow in Amazon rivers is characterized by seasonal droughts and floods with magnitudes varying from year to year. In the northern region of the Amazon, below average rainfall [*Aceituno*, 1988; *Zeng*, 1999; *Poveda et al*., 2001; *Zhou and Lau*, 2001; *Waylen and Poveda*, 2002; *Nobre et al*., 2006; *Aceituno et al*., 2009] and streamflow [*Marengo*, 1995; *Dettinger et al*., 2000; *Foley et al*., 2002; *Misir et al*., 2013] are commonly associated with El Niño events. Different from that pattern, the well-documented drought events of 2005 and 2010 unexpectedly affected western and southern regions of the Amazon and were associated with anomalous sea surface warming of the North Atlantic Ocean, not El Niño [*Marengo et al*., 2008a, 2008b, 2011; *Zeng et al*., 2008; *Espinoza et al*., 2011; *Lewis et al*., 2011; *Tomasella et al*., 2011, 2013]. Those recent droughts had unprecedented magnitude and caused significant economic and ecological impacts resulting from drying vegetation, and low river water levels. However, it is still unclear whether such recent, unprecedented events are part of spatial-temporal drought patterns that could be identified in historical streamflow observations.

Hydrological droughts in the Amazon result in significant impacts on regional economy and global climate. Low river levels may disrupt the regional river transportation system and isolate communities [*Marengo et al*., 2008b; *Lewis et al*., 2011; *Tomasella et al*., 2011, 2013]. Also, low soil moisture may restrict evapotranspiration from dense forest trees, increasing fire frequency, restricting biomass increase, and reducing the rate through which Amazonian trees capture and fix carbon [*Brown et al*., 2006; *Moran et al*., 2006; *Aragão et al*., 2007]. During intense droughts, the Amazon basin can even function as a carbon source, instead of a carbon sink, affecting the global carbon budget and atmospheric warming [*Phillips et al*., 2009; *Gatti et al*., 2014]. Hence, if droughts become more frequent as a result of climate change, a positive feedback is expected, as the drought-triggered reduced rate of carbon fixation might enhance global warming [*Costa and Foley*, 2000; *Cox et al*., 2000, 2004; *Costa et al*., 2007; *Betts and Silva Dias*, 2010; *Coe et al*., 2013]. That raises the importance of identifying possible new trends and patterns of hydrological droughts in the Amazon, and their relationships with climate and land use forcing conditions.

However, hydrological data in the Amazon are limited. The dense rain forest and the long river lengths impose difficulties on establishing conventional streamflow gauge networks [*Marengo*, 2006; *Espinoza Villar et al*., 2009a]. Most of the currently operational streamflow gauges were installed only after 1975, and they still are sparsely distributed and concentrated on the major rivers. That leaves large areas without historical hydrologic information that could be used to study past drought events. Also, gauge sites are not easily accessible, and thus, missing observations in the streamflow time series are common. Therefore, alternative methods need to be employed in order to take the most information out of the limited data available.

This paper employs probabilistic principal component analysis (PPCA) to derive spatial-temporal patterns of seasonal droughts within the Amazon basin. The method is used to extract the major modes of variability that

explain most of the variance of a drought indices data set, while accounting for the uncertainty in it [*Ilim and Raiko*, 2010]. Correlations among streamflow gauges and Monte Carlo simulations are used to estimate errors associated with missing data. Trend and uncertainty in the derived principal modes of variability are further explored as well as their correlation with climatic indices.

2. Methods

2.1. Data Sources

A set of 58 streamflow gauges maintained by the Brazilian National Water Agency (ANA) was selected from a pool of 405 existing gauges to characterize hydrological droughts in the Amazon basin. That selection was based on data availability and representativeness: all gauges cover the period from 1975 to 2013, are located on the major Amazon rivers, have daily streamflow observations covering at least 15 years and no more than 21% of gaps in the monthly time series. Gauge data consisted of consistency-checked, daily streamflow, computed from rating curves and daily water stage observations, and are publicly available online (http://www.snirh.gov.br/hidroweb/). Monthly streamflow time series are presented in the supporting information.

Two climatic indices were used for correlation analysis: the Niño 3.4 index, which indicates sea surface temperature (SST) anomalies over the Pacific Ocean, and a normalized, cross-equatorial SST gradient across the Atlantic Ocean (hereafter, the AGI). Niño 3.4 corresponds to monthly SST anomalies averaged over the area from 5° north to 5° south and from 170° to 120° west and is commonly used to identify El Niño–Southern Oscillation (ENSO) warm and cold phases (El Niño and La Niña, respectively). AGI was computed as the normalized difference between average SST over the North and South Atlantic Ocean sectors, taken as the area from 5° to 20° north, and from 60° to 30° west, and the area from 0° to 20° south, and from 30° west to 10° east, respectively. Annual anomalies were computed considering the typical annual cycles of the climatic indices, from June to May for Niño 3.4, and from April to March, for AGI. Niño 3.4 and SST data were obtained from the Climate Prediction Center from the National Oceanic and Atmospheric Administration, available online (http://www.cpc.ncep.noaa.gov/data/indices).

2.2. Drought Characterization

A seasonal drought is defined here as the event in which streamflow falls below the long-term mean of the monthly streamflow time series (Q_{LTM}). The magnitude of a drought event is computed as the accumulated deficit, i.e., the sum of the differences between Q_{LTM} and the monthly streamflow over the duration of the seasonal drought. When more than one drought event occurs in a given year, only the event with the larger magnitude is recorded, resulting in only one drought event per year. The obtained time series of magnitudes of seasonal droughts is normalized by its long-term means and standard deviations, resulting in the dry season drought index I_D. Similar calculations are performed for the wet season, i.e., the accumulated sum of differences between monthly streamflow and Q_{LTM} is computed and then normalized, resulting in the wet season drought index I_W. Note that both I_D and I_W refer to dry and wet seasons, respectively, in terms of streamflow, not rainfall.

Dry season index I_D takes on a positive value when drought magnitude is above its long-term mean (dry season streamflow is below average) and on a negative value otherwise. Accordingly, I_W takes on a positive value when the wet season streamflow is higher than average and negative value otherwise. Drought indices matrices with 39 rows (each of which corresponding to the period from 1975 to 2013) and 58 columns (each of which corresponding to a gauge) are constructed by concatenating the 58 times series of I_D and I_W for the application of PPCA.

2.3. Probabilistic Principal Component Analysis

Principal component analysis is commonly used to compute spatial-temporal patterns by deriving eigenvalues and eigenvectors of the covariance matrix of a drought index matrix. However, those computations require the absence of gaps in the matrix of drought indices, which is difficult to achieve with Amazon hydrologic data. If, in a specific gauge, the drought magnitude cannot be computed in a given year due to missing streamflow data, either that year or the gauge needs to be excluded from the analysis. Since nearly all gauges have at least one year with missing data, excluding those years or gauges would result in severe reduction of temporal or spatial coverage of the derived principal components, and increase in uncertainty. PPCA is an option to overcome that issue: instead of being excluded from the analysis, missing data are substituted

by statistical estimates, computed either from regression analysis or from observed data at the same gauge. That preserves a reasonable time extension of principal components and allows for uncertainty assessment.

First, gaps in time series of drought magnitudes in any given gauge are filled using linear regression equations in which the drought magnitudes at the nearest gauges, located on the same river or on a tributary, are the independent variables. The obtained linear regression equations include a residual error term ε that is assumed to be normally distributed with mean zero and constant, unknown variance, estimated as the sum of squared errors divided by $(n - m)$, where n is the number of streamflow gauges and m is the number of parameters (here, $n = 58$ and $m = 2$). When a single linear regression equation is not sufficient to fill all the gaps in a given time series, or when the coefficient of determination (r^2) is lower than 0.4, another nearby gauge is chosen to construct another linear regression, always choosing first the gauge with drainage area closer to that of the gauge of interest. When no nearby gauge has the required data for gap filling or when $r^2 < 0.4$, the missing value is estimated as the long-term mean of observed drought magnitudes for that gauge plus a random error δ, which is assumed to have zero mean, the same standard deviation of drought magnitudes at that gauge, and to be normally distributed.

Expected principal modes of variability are computed using conventional principal component analysis, after filling up all gaps in the data set and assuming zero the errors ε and δ. Then, a Monte Carlo simulation is employed to propagate the errors in the gap-filling process to the principal components. That iterative procedure starts by randomly generating 1000 sets of estimates of errors ε and δ, resulting in 1000 sets of time series of drought magnitudes and indices I_D and I_W for each gauge (1000 drought indices matrices). Finally, covariance matrices are extracted for each one of those 1000 matrices, allowing for the computation of 1000 sets of principal components loadings and scores. That large set of principal components allows for the computation of the mean and the standard deviation of the scores and loadings of the principal components, and evaluation of their uncertainty.

A truncation criterion is used to select the first principal components that explain most of the total variance of drought indices, following the "N rule" described by *Wilks* [2006]. The variances of each principal component are compared with corresponding variances obtained synthetically from random-generated data with the same dimensions (58 locations and 39 years), which are drawn from standard normal distributions. Original principal components are retained if their variances are above the 95% percentile of the distribution of synthetic eigenvalues.

An evaluation of whether the selected modes are distinguished from each other is performed by computing the error in the original variances. Assuming that the original drought indices are approximately multivariate normal distributions and no pair of variances are equal [*Wilks*, 2006], the standard deviation s_m of the mth eigenvalue λ_m is given by $s_m = \lambda_m (2/n)^{-0.5}$. If the difference of variances between the principal components is larger than one standard deviation, they can be considered statistically distinguishable.

2.4. Trend and Relationship With Climate Anomalies

The Mann-Kendall test [*Mann*, 1945; *Kendall*, 1975] is applied to verify the statistical significance of trends in dry and wet season indices computed at each streamflow gauge and in principal components, after checking for the absence of autocorrelation. The runs test [*Wald and Wolfowitz*, 1940] and the slope of regression lines are also used to check for such trends. Relationships with climate anomalies are assessed by computing Spearman rank correlation [*Spearman*, 1904] between I_D and I_W indices at each gauge and the annualized climatic indices Niño 3.4 and AGI, evaluated at the same or at the previous year. Rank correlations are also computed between the principal component time series associated with I_D and I_W indices, and climatic indices Niño 3.4 and AGI.

3. Results

3.1. Observed Droughts: Relationships With Climate Indices and Trends

Time series of observed I_D and I_W at Obidos, the most downstream gauge on the Amazon River, is presented in Figure 1. Many El Niño-related droughts that affected the Amazon River main stem are evident (1979, 1983, 1987, 1991, and 1997), though not always coinciding with low wet season indices I_W. Each drought had different spatial distribution of I_D, as noticed in the two most severe droughts recorded, 1997 and 2010,

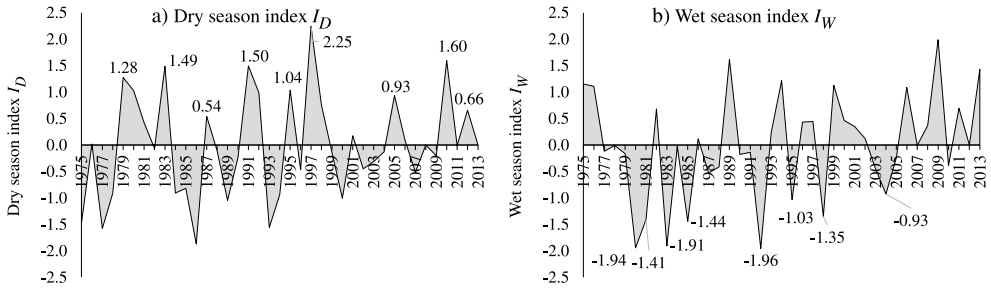

Figure 1. Time series of (a) dry and (b) wet season indices on the Amazon River at Obidos.

shown in Figure 2. While the 1997 drought impacted nearly all subbasins (except Madeira), the 2010 drought was more restricted to western and southern Amazon. Similar spatial patterns but with different drought magnitudes were observed for the droughts of 1983 and 2005, which are presented in the supporting information.

Spearman rank correlations between drought indices I_D and I_W at individual gauges, and climate indices Niño 3.4 and AGI highlight the connections of droughts in the Amazon to major climate forcing, as detailed presented in the supporting information. Consistent with previous studies, significant correlations between Niño 3.4 and drought indices are found on the Amazon River main stem and northern tributaries, which exhibit drier conditions (higher I_D and lower I_W) during or in the year following El Niño years. A few gauges at southern subbasins Madeira and Jurua, and even on the Amazon River, presented wetter conditions (lower I_D and higher I_W) during the El Niño year, but they also shifted to drier conditions in the following year. Differently, the effect of higher tropical Atlantic cross-equator SST differences (higher AGI) are observed in the same year: significant correlations suggest drier conditions (higher I_D and lower I_W) in association with AGI in many gauges on the Amazon River, Madeira, Purus, and Jurua subbasins, and a few gauges at Negro and northern tributaries (only lower I_W). Those conditions are even observed in the following year at a few gauges (Madeira, Purus, and Xingu subbasins). At the Negro subbasin, a few gauges indicated that higher AGI is actually associated with wetter dry seasons (lower I_D), even persisting in the following year.

According to the Mann-Kendall test, trends toward drier dry seasons (increasing I_D index) are significant at southern and western subbasins: at three out of 11 gauges in the Madeira river basin, at two out of nine gauges at the Tapajos River basin, and at other two gauges in the Xingu and Purus River basins. Significant trends toward drier wet seasons (decreasing I_W index) are also significant in Madeira River basin (four out of 11 gauges), and other two gauges at the Tapajos, Purus, and Xingu River basins. Opposite trends, toward less intense droughts (decreasing I_D index), are found in northern subbasins: at nine out of 10 gauges in the

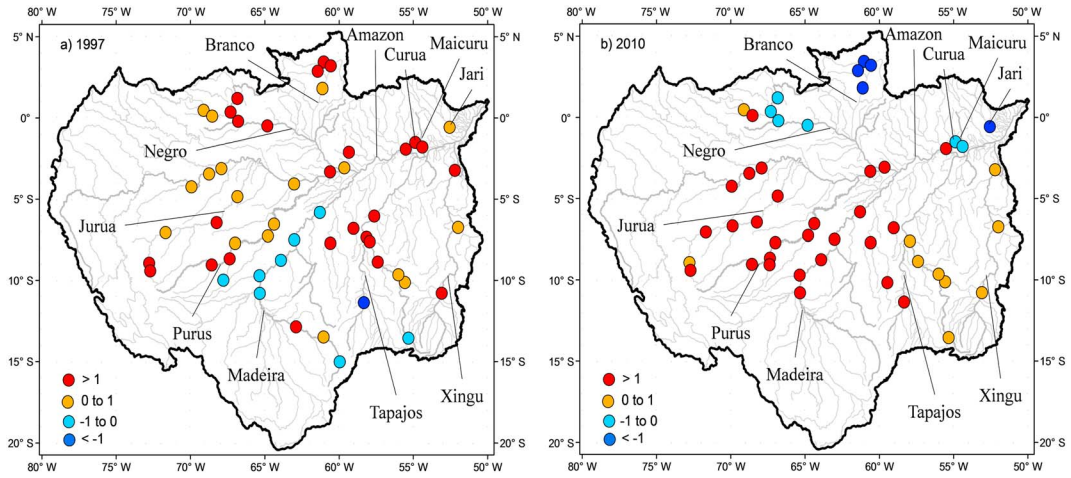

Figure 2. Major rivers and dry season drought indices I_D for the particular years of (a) 1997 and (b) 2010.

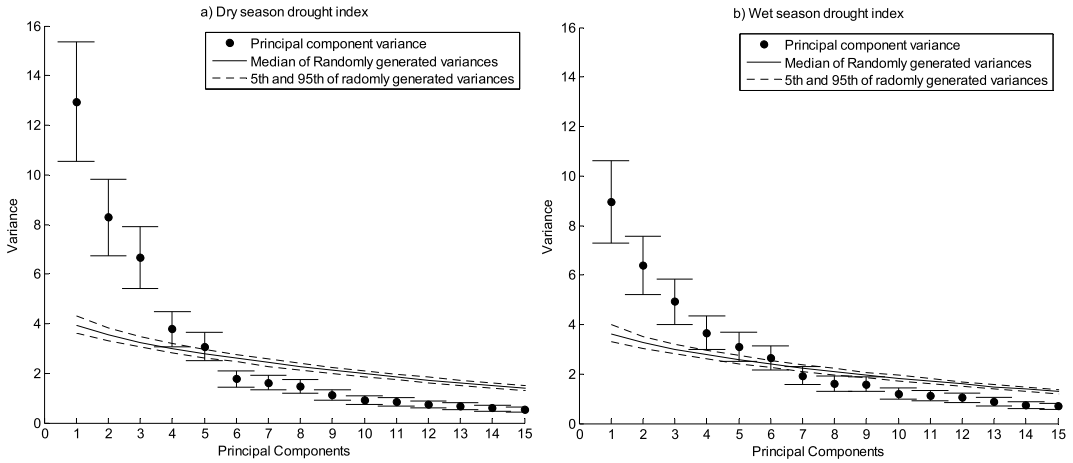

Figure 3. Variances and corresponding errors related to each principal component of (a) I_D and (b) I_W, and median of the variances obtained from randomly generated data, and corresponding 5th and 95th percentiles.

Negro River basin, and at one small northern tributary of the Amazon River. Consistently, trends toward wetter wet seasons (increasing I_W) are found in six out of 10 gauges in the Negro River basin and at three gauges on the Amazon River. Runs test only confirms the trends toward wetter dry and wet seasons in two gauges at the Negro River basin. Slopes of linear regressions are statistically significant toward more intense droughts in the Madeira, Purus, and Tapajos River basins, and less intense droughts in the Negro River basin, and at three gauges on the Amazon River. Tables summarizing the detected trends and results from statistical tests are presented in the supporting information.

Thus, this analysis of drought indices at individual gauges shows different spatial patterns: nearly all subbasins are affected during El Niño-related droughts (e.g., 1997), while western and southern subbasins are affected during extreme drought events such as in 2005 and 2010. Significant correlations indicate that drier conditions are associated with Niño 3.4 in northern (in the same year) and southern subbasins (in the following year) and drier conditions associated with AGI in southern subbasins (in the same year). Trend analysis suggests a shift toward drier conditions in south and western subbasins and toward wetter conditions at Negro subbasin.

3.2. Spatial-Temporal Patterns: Trends and Uncertainty

Figure 3 presents variances and corresponding errors (bars correspond to one standard deviation), and the median, 5th and 95th percentiles of variances obtained from randomly generated data for each principal component. The first three principal components of both I_D and I_W are significantly different from noise, as their variances are larger than what is obtained randomly. Estimated error in variances (error bars in Figure 3) indicate that the second and third principal components of I_D and all the principal components of I_W might not be statistically distinguishable from each other, due to the small sample size (58 gauges). The first three modes of variability of I_D explain 26%, 17%, and 14% of the total variance, respectively, totaling 57% of the total variance. Similarly, the first three modes of I_W explain 20%, 14%, and 11% of the total variance, respectively, jointly explaining 45% of the total variance.

The first two modes of variability of I_D are shown in Figure 4. The first mode (Figures 4a and 4c) is characterized by negative loadings in southern subbasins (especially Madeira, Purus, and upper Amazon River) and positive loadings in northern subbasins (Negro and Branco). In southern subbasins (negative loadings), severe droughts (positive I_D) occur when the score of the principal component is negative, and wetter-than-average droughts (negative I_D) occur when that score is positive. Accordingly, in northern subbasins (positive loadings), severe droughts (positive I_D) occur when the score of the principal component is positive, and moderate droughts (negative I_D) occur when the score of the principal component is negative. Thus, this first mode refers to a spatial pattern in which droughts are observed in southern subbasins, but not in northern ones, and vice versa. The interpretation of signs of drought indices, loadings, and scores is summarized in a table in the supporting information.

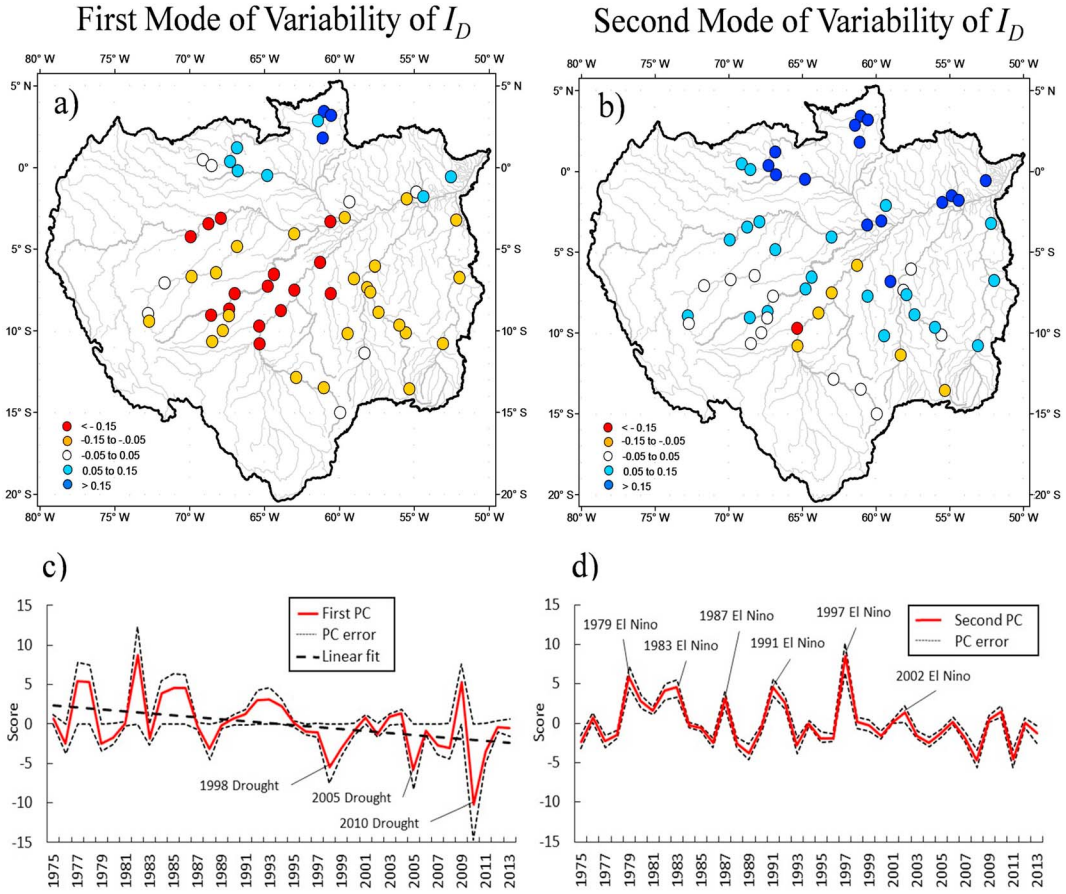

Figure 4. First and second modes of variability of the dry season drought index I_D. (a and b) Spatial pattern (loadings) is shown, and (c and d) time series (scores) is shown. Errors (one standard deviation, referred to as PC error, dashed black) and a linear fit to the first principal component scores (dashed, thick line) are also shown.

Droughts of 1998, 2005, and 2010 are indicated as negative scores in the time series of this first principal component (Figure 4c). There is a trend toward negative scores, which means increasing drought magnitude in southern subbasins, not followed by droughts in northern subbasins. That trend is statistically significant at 5% level according to results from the Mann-Kendall test, the runs test ($p = 0.016$), and the significance of the slope of the linear regression (between -0.03 and -0.22, for a 95% confidence interval).

The second principal mode (Figures 4b and 4d) is characterized by positive loadings in almost all gauges (especially Negro and Branco River basins), except in the Madeira River and two headwaters of southern subbasins. Differently from the first mode, that pattern indicates widespread drought (positive loadings and I_D) and wetter conditions at Madeira subbasin when the score of the principal component is also positive; and wetter dry seasons (positive loadings and negative I_D) and drier conditions at Madeira subbasin when that score is negative. Thus, while the first mode shows droughts restricted to southern subbasins (coincident with wetter conditions in northern subbasins), the second mode shows widespread drought (or widespread wetter conditions), except in the Madeira River. Time series of scores of this second mode (Figure 4d) shows marked positive high values coincident with El Niño years of 1979, 1983, 1987, 1991, 1997, and 2002. No significant trend is found in this second mode.

The first principal mode of I_W (presented in the supporting information) is characterized again by a marked distinction between northern and southern subbasins. There are positive loadings in southern subbasins, especially on the Madeira River and negative loadings in the northern subbasins, northeast tributaries, and on the Amazon River main stem. Time series of this first mode presents a trend (although less pronounced) toward negative scores, which means more intense wet seasons in northern subbasins and drier wet seasons

in the southern subbasins. That trend is statistically significant according to the Mann-Kendall test and the slope of the linear regression (slope between −0.20 and −0.05), but not according to the runs test ($p = 0.647$).

Therefore, the two major modes of variability of I_D and I_W differ according to each subbasin. In the first mode, southern and western subbasins are drier than normal at the same time when northern subbasins are wetter than normal, and vice versa. Trend analysis suggests that drought intensity associated with that spatial pattern is increasing with time. In the second mode, drier-than-normal conditions occur in all subbasins, except Madeira, but there is no significant trend in drought intensity.

3.3. Relation With Climatic Indices

Spearman rank correlation coefficients between Niño 3.4, AGI, and the first two principal component time series are considered here. Niño 3.4 is significantly correlated with the first and second principal components of I_D, with correlations of 0.49 ($p < 0.01$) and 0.33 ($p = 0.04$), respectively. Those correlations are positive, indicating that El Niño events (warm Pacific SST, positive Niño 3.4) are associated with positive values in those principal component scores (see Figures 4c and 4d). In the first mode, that means more severe droughts in the northern subbasins (positive I_D and positive loadings in Figure 4a) and less severe droughts in southern subbasins (negative I_D and negative loadings in Figure 4a). Thus, in this mode, El Niño affects droughts only restricted to northern subbasins and does not explain the trend toward more intense droughts in southern subbasins (represented by negative scores in Figure 4c). In the second mode, El Niño largely explains droughts affecting both northern and southern subbasins, except the Madeira River.

The AGI index is also significantly correlated to the first and second principal components of I_D, with correlations of −0.29 ($p = 0.08$) and 0.31 ($p = 0.05$), respectively. In the first mode, the correlation is negative, and thus, a positive north-south Atlantic SST difference (with warm north Atlantic SST) is associated with negative values of scores in Figure 4c. Those negative values mean more severe droughts in the southern subbasins (positive I_D and negative loadings in Figure 4a) and less severe droughts restricted to northern subbasins (negative I_D and positive loadings in Figure 4a). Thus, AGI index does explain the trend toward more intense droughts in southern subbasins. In the second mode, the correlation with AGI is positive, indicating that a positive north-south Atlantic SST difference is now associated with also positive values of scores in Figure 4d. Those positive values mean more severe droughts in both northern and southern subbasins (positive I_D and positive loadings in Figure 4b), except the Madeira subbasin (negative I_D and negative loadings in Figure 4b).

Correlations between the principal components of I_W and Niño 3.4 or AGI are not statistically significant, meaning that neither Pacific nor Atlantic SST anomalies explain the variability of wet season indices. Thus, neither of them explains the trend toward wetter wet seasons in northern subbasins, detected in the first mode of variability of I_W.

4. Discussion and Conclusion

Two main modes of spatial-temporal variability of drought indices computed from streamflow observations within the Amazon basin are identified. The first mode exhibits a dual dry-wet pattern, in which southern-western subbasins are dry at the same time when northern subbasins are wet (or vice versa), while the second mode refers to widespread drought (or wet conditions) affecting nearly all subbasins but the Madeira River. Both modes are significantly correlated with Niño 3.4, which is in agreement with many previous studies that have identified ENSO as a major driver of interannual variability in rainfall and streamflow in the Amazon [*Ropelewski and Halpert*, 1987; *Aceituno*, 1988; *Marengo et al*., 1993; *Zeng*, 1999; *Dettinger et al*., 2000; *Foley et al*., 2002; *Espinoza Villar et al*., 2009a, 2009b]. However, in the first mode, the correlations imply that El Niño partially explains droughts that are restricted to northern subbasins (where loadings are positive), in agreement with aforementioned studies, that linked El Niño to reduced rainfall and streamflow in those subbasins. Differently, the second mode reveals that ENSO can also jointly affect northern, southern, and western subbasins, notably during strong El Niño years (e.g., 1997). The exception of the Madeira River might be related to the more frequent intrusion of cold fronts coming from the south during strong El Niño years [*Marengo et al*., 1997].

The significant correlation between AGI and the first mode of variability of I_D highlights that tropical Atlantic SST anomalies are linked to severe droughts affecting western and southern subbasins, as pointed out in previous investigations on the recent events of 2005 and 2010 [*Marengo et al*., 2008a, 2008b, 2011]. That

association is also present in the second mode, characterized by widespread drought. However, significant trends (toward negative scores) are only found in the first mode, suggesting intensification of the spatial pattern characterized by more intense droughts in southern subbasins and wetter conditions in northern subbasins. Analysis of trends at individual gauges confirm drying trends at specific gauges in Madeira, Purus, Xingu, and Tapajos subbasins, and wetting trends in Negro subbasin. Similar trends have been detected in previous studies that assessed minimum, maximum, and mean monthly runoff, in association with trends in rainfall and changes in atmospheric circulation [*Espinoza Villar et al*., 2009a]. Drying trends are also in agreement with North Atlantic warming and consequent reduction of water vapor transport toward western subbasins [*Espinoza et al*., 2011]. In addition, such trends are in agreement with previous studies that have projected increase in duration and deficit volume of droughts due to climate change in Madeira, Jurua, and Amazon rivers, although there is uncertainty on changes in low streamflow [*van Huijgevoort et al*., 2014]. Indeed, drying trends in that part of the Amazon basin are projected by many studies as a consequence of climate change [*Neelin*, 2003; *Malhi et al*., 2008; *Nobre et al*., 2009; *Arnell and Gosling*, 2013; *van Huijgevoort et al*., 2014], deforestation [*Nobre et al*., 1991; *Costa and Pires*, 2010], combined deforestation and atmospheric warming [*Costa and Foley*, 2000], and even North Atlantic warming due to decreased aerosol pollution [*Cox et al*., 2008]. Interestingly, few studies have detected decreased monthly rainfall in western and central Amazon [*Paiva and Clarke*, 1995; *Espinoza Villar et al*., 2009a, 2009b], and many have not identified trends in seasonal or annual rainfall or streamflow [*Marengo*, 1995; *Marengo and Tomasella*, 1998; *Costa and Foley*, 1999; *Malhi and Wright*, 2004]. The present study does not contradict those studies, as it refers to drought, not total rainfall (or streamflow). For example, drought indices can increase due to changes in rainfall timing even if no change occurs in total rainfall. Additionally, some previous studies have projected decreased rainfall in northern Amazon, as a consequence of intensification of ENSO [*Coelho and Goddard*, 2009], and increased streamflow due to deforestation in southern subbasins [*Coe et al*., 2009]. The results here apparently contradict those studies, as they indicate trends toward wetting conditions in Negro subbasin and drying trends in some southern and western subbasins.

Causes of the trends in drought indices and principal components might be quite distinct in each subbasin. For example, rainfall over the Madeira River basin have reduced [*Paiva and Clarke*, 1995; *Espinoza Villar et al*., 2009a] while the duration of dry season has increased [*Costa and Pires*, 2010], and those factors could have produced the trend toward drought intensification. Second, the Tapajos River drains southern parts of the Amazon basin that had been subjected to intense deforestation, as 20% of its areas had been deforested by 2000 [*Cardille and Foley*, 2003; *Coe et al*., 2009]. That change in land cover might alter the regional climate, leading to reduction of rainfall recycling [*Nobre et al*., 1991; *Coe et al*., 2009] and increasing of dry season duration [*Costa and Pires*, 2010], both resulting in intensification of drought indices. Since such local hydrological processes might modulate the increase in drought intensity, further investigations based on field hydrologic measurements are needed to determine what is causing the identified trends.

Acknowledgments
The first author gratefully acknowledge the support received by the Brazilian Coordination for Improvement of Higher Education Personnel (CAPES) and Fulbright, through its doctorate scholarship program (grant BEX 2118/08-4), and the National Water Agency (ANA), through its advanced capacitation program. The data used are listed in the references and can be directly obtained with the first author upon request over e-mail.

References

Aceituno, P. (1988), On the functioning of the Southern Oscillation in the South American sector. Part I: Surface climate, *Mon. Weather Rev.*, *116*(3), 505–524, doi:10.1175/1520-0493(1988)116<0505:OTFOTS>2.0.CO;2.

Aceituno, P., M. del Rosario Prieto, M. E. Solari, A. Martínez, G. Poveda, and M. Falvey (2009), The 1877–1878 El Niño episode: Associated impacts in South America, *Clim. Change*, *92*(3–4), 389–416, doi:10.1007/s10584-008-9470-5.

Aragão, L. E. O. C., Y. Malhi, R. M. Roman-Cuesta, S. Saatchi, L. O. Anderson, and Y. E. Shimabukuro (2007), Spatial patterns and fire response of recent Amazonian droughts, *Geophys. Res. Lett.*, *34*, L07701, doi:10.1029/2006GL028946.

Arnell, N. W., and S. N. Gosling (2013), The impacts of climate change on river flow regimes at the global scale, *J. Hydrol.*, *486*, 351–364, doi:10.1016/j.jhydrol.2013.02.010.

Betts, A. K., and M. A. F. Silva Dias (2010), Progress in understanding land-surface-atmosphere coupling from LBA research, *J. Adv. Model. Earth Syst.*, *2*, 6, doi:10.3894/JAMES.2010.2.6.

Brown, I. F., W. Schroeder, A. Setzer, M. De Los Rios Maldonado, N. Pantoja, A. Duarte, and J. Marengo (2006), Monitoring fires in southwestern Amazonia rain forests, *Eos Trans. Am. Geophys. Union*, *87*(26), 253–259, doi:10.1029/2006EO260001.

Cardille, J. A., and J. A. Foley (2003), Agricultural land-use change in Brazilian Amazônia between 1980 and 1995: Evidence from integrated satellite and census data, *Remote Sens. Environ.*, *87*(4), 551–562, doi:10.1016/j.rse.2002.09.001.

Coe, M. T., M. H. Costa, and B. S. Soares-Filho (2009), The influence of historical and potential future deforestation on the stream flow of the Amazon River—Land surface processes and atmospheric feedbacks, *J. Hydrol.*, *369*(1–2), 165–174, doi:10.1016/j.jhydrol.2009.02.043.

Coe, M. T., et al. (2013), Deforestation and climate feedbacks threaten the ecological integrity of south–southeastern Amazonia, *Philos. Trans. R. Soc. B Biol. Sci.*, *368*(1619), doi:10.1098/rstb.2012.0155.

Coelho, C. A. S., and L. Goddard (2009), El Niño–induced tropical droughts in climate change projections, *J. Clim.*, *22*(23), 6456–6476, doi:10.1175/2009JCLI3185.1.

Costa, M. H., and G. F. Pires (2010), Effects of Amazon and Central Brazil deforestation scenarios on the duration of the dry season in the arc of deforestation, *Int. J. Climatol.*, *30*(13), 1970–1979, doi:10.1002/joc.2048.

Costa, M. H., and J. A. Foley (1999), Trends in the hydrologic cycle of the Amazon Basin, *J. Geophys. Res.*, *104*(D12), 14,189–14,198, doi:10.1029/1998JD200126.

Costa, M. H., and J. A. Foley (2000), Combined effects of deforestation and doubled atmospheric CO_2 concentrations on the climate of Amazonia, *J. Clim.*, *13*(1), 18–34, doi:10.1175/1520-0442(2000)013<0018:CEODAD>2.0.CO;2.

Costa, M. H., S. N. M. Yanagi, P. J. O. P. Souza, A. Ribeiro, and E. J. P. Rocha (2007), Climate change in Amazonia caused by soybean cropland expansion, as compared to caused by pastureland expansion, *Geophys. Res. Lett.*, *34*, L07706, doi:10.1029/2007GL029271.

Cox, P. M., R. A. Betts, C. D. Jones, S. A. Spall, and I. J. Totterdell (2000), Acceleration of global warming due to carbon-cycle feedbacks in a coupled climate model, *Nature*, *408*(6809), 184–187, doi:10.1038/35041539.

Cox, P. M., R. A. Betts, M. Collins, P. P. Harris, C. Huntingford, and C. D. Jones (2004), Amazonian forest dieback under climate-carbon cycle projections for the 21st century, *Theor. Appl. Climatol.*, *78*(1–3), 137–156, doi:10.1007/s00704-004-0049-4.

Cox, P. M., P. P. Harris, C. Huntingford, R. A. Betts, M. Collins, C. D. Jones, T. E. Jupp, J. A. Marengo, and C. A. Nobre (2008), Increasing risk of Amazonian drought due to decreasing aerosol pollution, *Nature*, *453*(7192), 212–215, doi:10.1038/nature06960.

Dettinger, M. D., D. R. Cayan, G. J. Mccabe, and J. A. Marengo (2000), Multiscale streamflow variability associated with El Niño/Southern Oscillation, in *El Niño and the Southern Oscillation—Multiscale Variability and Global and Regional Impacts*, pp. 113–146, Cambridge Univ. Press.

Espinoza, J. C., J. Ronchail, J. L. Guyot, C. Junquas, P. Vauchel, W. Lavado, G. Drapeau, and R. Pombosa (2011), Climate variability and extreme drought in the upper Solimões River (western Amazon Basin): Understanding the exceptional 2010 drought, *Geophys. Res. Lett.*, *38*, L13406, doi:10.1029/2011GL047862.

Espinoza Villar, J. C., J. L. Guyot, J. Ronchail, G. Cochonneau, N. Filizola, P. Fraizy, D. Labat, E. de Oliveira, J. J. Ordonez, and P. Vauchel (2009a), Contrasting regional discharge evolutions in the Amazon basin (1974–2004), *J. Hydrol.*, *375*(3–4), 297–311, doi:10.1016/j.jhydrol.2009.03.004.

Espinoza Villar, J. C., J. Ronchail, J. L. Guyot, G. Cochonneau, F. Naziano, W. Lavado, E. De Oliveira, R. Pombosa, and P. Vauchel (2009b), Spatio-temporal rainfall variability in the Amazon basin countries (Brazil, Peru, Bolivia, Colombia, and Ecuador), *Int. J. Climatol.*, *29*(11), 1574–1594, doi:10.1002/joc.1791.

Foley, J. A., A. Botta, M. T. Coe, and M. H. Costa (2002), El Niño–Southern oscillation and the climate, ecosystems and rivers of Amazonia, *Global Biogeochem. Cycles*, *16*(4), 1132, doi:10.1029/2002GB001872.

Gatti, L. V., et al. (2014), Drought sensitivity of Amazonian carbon balance revealed by atmospheric measurements, *Nature*, *506*(7486), 76–80, doi:10.1038/nature12957.

Ilim, A., and T. Raiko (2010), Practical approaches to principal component analysis in the presence of missing values, *J. Mach. Learn. Res.*, *11*, 1957–2000.

Kendall, M. G. (1975), *Rank Correlation Methods*, 4th ed., Charles Griffin, London.

Lewis, S. L., P. M. Brando, O. L. Phillips, G. M. F. van der Heijden, and D. Nepstad (2011), The 2010 Amazon drought, *Science*, *331*(6017), 554–554, doi:10.1126/science.1200807.

Malhi, Y., and J. Wright (2004), Spatial patterns and recent trends in the climate of tropical rainforest regions, *Philos. Trans. R. Soc. B Biol. Sci.*, *359*, 311–329.

Malhi, Y., J. T. Roberts, R. A. Betts, T. J. Killeen, W. Li, and C. A. Nobre (2008), Climate change, deforestation, and the fate of the Amazon, *Science*, *319*(5860), 169–172, doi:10.1126/science.1146961.

Mann, H. B. (1945), Nonparametric tests against trend, *Econometrica*, *13*, 245–259.

Marengo, J. A. (1995), Variations and change in South American streamflow, *Clim. Change*, *31*(1), 99–117, doi:10.1007/BF01092983.

Marengo, J. A. (2006), On the hydrological cycle of the Amazon basin: A historical review and current state-of-the-art, *Rev. Bras. Meteorol.*, *21*(3), 1–19.

Marengo, J. A., and J. Tomasella (1998), Trends in streamflow and rainfall in tropical South America: Amazonia, eastern Peru, and north-western Peru, *J. Geophys. Res.*, *103*(2), 1775–1783, doi:10.1029/97JD02551.

Marengo, J. A., L. M. Druyan, and S. Hastenrath (1993), Observational and modelling studies of Amazonia interannual climate variability, *Clim. Change*, *23*(3), 267–286, doi:10.1007/BF01091619.

Marengo, J. A., A. Cornejo, P. Satyamurty, C. Nobre, and W. Sea (1997), Cold surges in tropical and extratropical South America: The strong event in June 1994, *Mon. Weather Rev.*, *125*(11), 2759–2786, doi:10.1175/1520-0493(1997)125<2759:CSITAE>2.0.CO;2.

Marengo, J. A., C. A. Nobre, J. Tomasella, M. F. Cardoso, and M. D. Oyama (2008a), Hydro-climatic and ecological behaviour of the drought of Amazonia in 2005, *Philos. Trans. R. Soc. B Biol. Sci.*, *363*(1498), 1773–1778, doi:10.1098/rstb.2007.0015.

Marengo, J. A., C. A. Nobre, J. Tomasella, M. D. Oyama, G. Sampaio de Oliveira, R. de Oliveira, H. Camargo, L. M. Alves, and I. F. Brown (2008b), The drought of Amazonia in 2005, *J. Clim.*, *21*(3), 495–516, doi:10.1175/2007JCLI1600.1.

Marengo, J. A., J. Tomasella, L. M. Alves, W. R. Soares, and D. A. Rodriguez (2011), The drought of 2010 in the context of historical droughts in the Amazon region, *Geophys. Res. Lett.*, *38*, L12703, doi:10.1029/2011GL047436.

Misir, V., D. S. Arya, and A. R. Murumkar (2013), Impact of ENSO on river flows in Guyana, *Water Resour. Manage.*, *27*(13), 4611–4621, doi:10.1007/s11269-013-0430-0.

Moran, E. F., R. Adams, B. Bakoyéma, S. T. Fiorini, and B. Boucek (2006), Human strategies for coping with El Niño related drought in Amazônia, *Clim. Change*, *77*(3–4), 343–361, doi:10.1007/s10584-005-9035-9.

Neelin, J. D. (2003), Tropical drought regions in global warming and El Niño teleconnections, *Geophys. Res. Lett.*, *30*(24), 2275, doi:10.1029/2003GL018625.

Nobre, C. A., P. J. Sellers, and J. Shukla (1991), Amazonian deforestation and regional climate change, *J. Clim.*, *4*(10), 957–988, doi:10.1175/1520-0442(1991)004<0957:ADARCC>2.0.CO;2.

Nobre, P., J. A. Marengo, I. F. A. Cavalcanti, G. Obregon, V. Barros, I. Camilloni, N. Campos, and A. G. Ferreira (2006), Seasonal-to-decadal predictability and prediction of South American climate, *J. Clim.*, *19*(23), 5988–6004, doi:10.1175/JCLI3946.1.

Nobre, P., M. Malagutti, D. F. Urbano, R. A. F. de Almeida, and E. Giarolla (2009), Amazon deforestation and climate change in a coupled model simulation, *J. Clim.*, *22*(21), 5686–5697, doi:10.1175/2009JCLI2757.1.

Paiva, E. M. C. D., and R. T. Clarke (1995), Time trends in rainfall records in Amazonia, *Bull. Am. Meteorol. Soc.*, *76*(11), 2203–2209, doi:10.1175/1520-0477(1995)076<2203:TTIRRI>2.0.CO;2.

Phillips, O. L., et al. (2009), Drought sensitivity of the Amazon rainforest, *Science*, *323*(5919), 1344–1347, doi:10.1126/science.1164033.

Poveda, G., A. Jaramillo, M. M. Gil, N. Quiceno, and R. I. Mantilla (2001), Seasonally in ENSO-related precipitation, river discharges, soil moisture, and vegetation index in Colombia, *Water Resour. Res.*, *37*(8), 2169–2178, doi:10.1029/2000WR900395.

Ropelewski, C., and M. S. Halpert (1987), Global and regional scale precipitation patterns associated with the El Niño/Southern Oscillation, *Mon. Weather Rev.*, 1606–1626.

Spearman, C. (1904), The proof and measurement of association between two things, *Am. J. Psychol.*, *15*(1), 72–101, doi:10.2307/1412159.
Tomasella, J., L. S. Borma, J. A. Marengo, D. A. Rodriguez, L. A. Cuartas, C. A. Nobre, and M. C. R. Prado (2011), The droughts of 1996–1997 and 2004–2005 in Amazonia: Hydrological response in the river main-stem, *Hydrol. Process.*, *25*(8), 1228–1242, doi:10.1002/hyp.7889.
Tomasella, J., P. F. Pinho, L. S. Borma, J. A. Marengo, C. A. Nobre, O. R. F. O. Bittencourt, M. C. R. Prado, D. A. Rodriguez, and L. A. Cuartas (2013), The droughts of 1997 and 2005 in Amazonia: Floodplain hydrology and its potential ecological and human impacts, *Clim. Change*, *116*(3–4), 723–746, doi:10.1007/s10584-012-0508-3.
Van Huijgevoort, M. H. J., H. A. J. van Lanen, A. J. Teuling, and R. Uijlenhoet (2014), Identification of changes in hydrological drought characteristics from a multi-GCM driven ensemble constrained by observed discharge, *J. Hydrol.*, *512*, 421–434, doi:10.1016/j.jhydrol.2014.02.060.
Wald, A., and J. Wolfowitz (1940), On a test whether two samples are from the same population, *Ann. Math. Stat.*, *11*(2), 147–162, doi:10.1214/aoms/1177731909.
Waylen, P., and G. Poveda (2002), El Niño–Southern Oscillation and aspects of western South American hydro-climatology, *Hydrol. Process.*, *16*(6), 1247–1260, doi:10.1002/hyp.1060.
Wilks, D. S. (2006), *Statistical Methods in the Atmospheric Sciences*, 2nd ed., Elsevier Inc., Burlington, Mass.
Zeng, N. (1999), Seasonal cycle and interannual variability in the Amazon hydrologic cycle, *J. Geophys. Res.*, *104*(D8), 9097–9106, doi:10.1029/1998JD200088.
Zeng, N., J.-H. Yoon, J. A. Marengo, A. Subramaniam, C. A. Nobre, A. Mariotti, and J. D. Neelin (2008), Causes and impacts of the 2005 Amazon drought, *Environ. Res. Lett.*, *3*(1), 014002, doi:10.1088/1748-9326/3/1/014002.
Zhou, J., and K.-M. Lau (2001), Principal modes of interannual and decadal variability of summer rainfall over South America, *Int. J. Climatol.*, *21*(13), 1623–1644, doi:10.1002/joc.700.